

## “3d Heat Transfer Analysis And Numerical Modeling Of Lens<sup>tm</sup> Process For Thin Wall By Using Stainless Steel 304”

Chirag P. Patel<sup>1</sup>, Prof. R.I. Patel<sup>2</sup>

<sup>1,2</sup>( Department Of Mechanical Engineering, Government Engineering College, Dahod/ GTU, India

**Abstract :** Laser Engineered Net Shaping (LENS<sup>TM</sup>) is a rapid-manufacturing procedure that involves complex thermal, mechanical, and metallurgical interactions. The finite element method (FEM) may be used to accurately model this process, allowing for optimized selection of input parameters, and, hence, the fabrication of components with improved Thermo-mechanical properties. In this study the commercial FEM code ANSYS is used to predict the thermal histories, total deformation, von-misses stress and shear stress generated in straight wall and substrate of stainless steel 304. The computational results are compared with experimental measurements for validation.

**Keywords:** Laser engineering net shaping, FEM, total deformation, von-misses stress and shear stress , Element birth and death technique.

### I. INTRODUCTION

Laser Engineered Net Shaping (LENS<sup>TM</sup>) is a rapid manufacturing technology developed by Sandia National Laboratories (SNL) that combines features of powder injection and laser welding toward component fabrication. Several aspects of LENS<sup>TM</sup> are similar to those of single-step laser cladding. However, whereas laser cladding is primarily used to bond metallic coatings to the surfaces of parts that have already been produced with traditional methods<sup>[1]</sup>, LENS<sup>TM</sup> involves the complete fabrication of three-dimensional, solid metallic components through layer by layer deposition of melted powder metal. In this process, a laser beam is directed onto the surface of a metallic substrate to create a molten pool. Powder metal is then propelled by an inert gas, such as argon or nitrogen through

### II. Literature Review

Keicher *et al.*<sup>[5]</sup> evaluated the effects of process parameters on multi-layer deposition of laser-melted powder Inconel® 625 in a process similar to both laser cladding and LENS<sup>TM</sup>. The group initially examined various parameters, including laser irradiance, stage translation speed, powder flow rate, powder particle size, and the size of each Z-directional increment between layers and their effect on heat affected zone (HAZ) size generated during the build. The HAZ was defined in this study as the melted region below the surface of the substrate and was examined post-build via metallographic analysis. Khalen and Kar<sup>[10]</sup> performed an investigation into the effects of a several parameters on the resulting yield strength of AISI 304 stainless steel thin plates in process identical to LENS<sup>TM</sup> termed laser-aided direct rapid manufacturing (LADRM).

converging nozzles into the molten pool. Depending upon the alignment of the nozzle focal point with respect to that of laser, then powder is then melted either mid-stream or as it enters the pool. As the laser source moves away, the molten material then quickly cools by conduction through the substrate, leaving a solidified deposit. The substrate is located on a 3 or 5-axis stage capable of translating in the X and Y-directions. Initially, a 3-D CAD model is created to represent the geometry of a desired component. The CAD model is then converted to a faceted geometry composed of multiple slices used to direct the movement of the X-Y stage where each slice represents a single layer of deposition. During the build, the powder-nozzle/laser/stage system first traces a 2-D outline of the cross section represented by each slice I the X-Y plane and then proceeds to fill this area with an operator-specified rastering pattern.

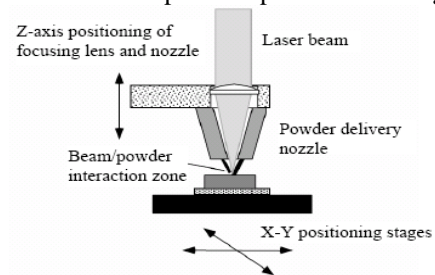


Figure 1 : Schematic of LENS<sup>TM</sup> deposition process

The laser/nozzle assembly then ascends in the Z-direction so that the next layer can be added. This process is repeated for consecutive layers, until completion of the 3-D component<sup>[2]</sup>. This feature is illustrated schematically in Figure 1

This team sought to generate a range of input parameter values within which components with acceptable mechanical properties could be deposited. Their approach involved using the Buckingham Π-Theorem to express the process variables associated with heat transfer and powder mass flux in terms of 14 dimensionless parameters. Rangaswamy *et al.*<sup>[11,12]</sup> sought to experimentally measure residual stresses in LENS<sup>TM</sup> deposits using the neutron diffraction method, the details of which are discussed in next Section. The measurements were performed on LENS<sup>TM</sup>-produced rectangular plates of AISI 316. The neutron data was collected at several points methodically distributed within the geometry of the samples, to provide a map of the stress distribution then calculated the axial components of residual stress through Hooke's law. Each stress component was then plotted against position within the plate, first, along the height (Z direction) on the sample vertical centerline, and

next, along the width (Y-direction) on the plate horizontal centre line. Wang and Felicelli<sup>[15]</sup> next performed a parametric study similar to that done by Hofmeister *et al.*<sup>[8]</sup> to determine if the same trends in cooling rates and thermal gradients were observable for different laser power. He repeated the previous simulation using five power intensity values, revealing that the temperature gradient at the edge of the molten pool increases substantially with laser power, while the cooling rate decreases. The resulting plots are shown in Figure 8 where A0 indicates power intensity. Neela and De<sup>[16]</sup> to study the effects of translation speed and laser power on the resulting temperature profiles using the general purpose FE package, ABAQUS® 6.6. The researchers used an element Activation/deactivation similar to those previously to model the deposition of a thin plate of AISI 316 with temperature-dependent thermal conductivity and specific heat according to a linear, and quadratic relation, respectively. Deus and Mazumder<sup>[17]</sup> attempted to predict the residual stresses resulting from a laser cladding deposition of C95600 copper alloy onto an AA333 aluminium alloy substrate. Since residual stresses would be generated by the heterogeneous thermal expansions of the deposited and substrate materials, accurate stress calculations would also require accurate prediction of the temperature fields created during the build. Labudovic *et al.*<sup>[18]</sup> to predict residual stresses in a process identical to LENS<sup>TM</sup> termed the direct laser metal powder deposition process. A 3-D coupled model was implemented through the FE package ANSYS® for the deposition of a 50 mm x 20 mm x 10 mm thin plate of MONEL 400 onto a substrate of AISI 1006. The deposition was modelled with an ANSYS® element activation option similar to those already presented. Energy input density was modelled as a moving Gaussian distribution through the ANSYS® Parametric Design Language subroutine. The constitutive model was a temperature-dependent visco-plastic model, in which viscous effects were neglected by ignoring it the associated term in the equation of state.

### III. Thermal modeling

#### 3.1 Temperature Distribution

In the LENS process, a moving laser beam strikes on the substrate cause the powder and a portion to melt. The melted parts solidify again after cooling. By solving the three-dimensional heat conduction equation in the substrate, the transient temperature field can be obtained. The heat conduction equation with no source term is:

$$\frac{\partial}{\partial x} \left( k \frac{\partial T}{\partial x} \right) + \frac{\partial}{\partial y} \left( k \frac{\partial T}{\partial y} \right) + \frac{\partial}{\partial z} \left( k \frac{\partial T}{\partial z} \right) = \rho c_p \left( \frac{\partial T}{\partial t} \right) \quad \dots(1)$$

Where k is the thermal conductivity, T is the temperature, ρ is the density, p c is the specific heat and t is the time. The left term of Eq. (1) depicts the conductive heat transfer in the space while the right term of Eq. (1) refers to the imposed heat flux at a point of the clad. The heat conduction equation must be subject to the following boundary conditions: The imposed heat flux will

correspond to the power density of the laser beam. Assuming an uniform-distributed laser beam, we have:

$$Q(x, y, z, t) = \frac{Pa}{\pi r_0^2} \quad \dots\dots(2)$$

where P is the power of laser source, a is the absorptivity of clad material and r<sub>0</sub> is the radius of laser beam. The heat conduction equation must be subject to the following boundary conditions: Convection:

$$-k\nabla T = h(T - T_0) \quad \dots\dots(3)$$

Radiation:

$$-k\nabla T = \epsilon\sigma(T^4 - T_0^4) \quad \dots\dots(4)$$

Where h is the convective heat transfer coefficient, ε is the emissivity, σ is the Stephan-Boltzmann constant and T<sub>0</sub> is the ambient temperature. In addition, the following initial condition should be satisfied

$$T(x, y, z, 0) = T_0 \quad \text{and} \quad T(x, y, z, \infty) = T_0 \quad \dots\dots(5)$$

#### 3.2 Stress Analysis

In this case, no body forces or surface tractions are applied and the only load is from the transient thermal field. The strong temperature gradients induced by laser beam causes thermal strain which lead the work piece to yield. The total strain is written as:

$$\epsilon_{ij} = \epsilon_{ij}^e + \epsilon_{ij}^p + \epsilon_{ij}^{th} \quad \dots\dots\dots(6)$$

Where the components refer to elastic, plastic and thermal strain, respectively. The elastic and thermal strains are expressed as :

$$\epsilon_{ij}^E = \frac{1+\nu}{E} \sigma_{ij} - \frac{\nu}{E} \sigma_{kk} \delta_{ij} \quad \dots\dots\dots(7)$$

And

$$\epsilon_{ij}^T = \alpha(T - T_0) \delta_{ij} \quad \dots\dots\dots(8)$$

To calculate the plastic strain, kinematic hardening, together with Von Mises yield criterion is assumed.

#### 3.3 Modeling assumptions

The assumptions during the thermal and structural modeling of the LENS process are as follows:

The substrate is initially at room temperature (20°C). The boundary condition around the substrate is the convection heat transfer with a constant coefficient. The heat flux is moving and it has uniform distribution on the activated elements.

The activated elements of the molten pool are at the melting temperature. The convective redistribution of heat in the molten pool is considered. The substrate is assumed to be stress free at the beginning of the process. The substrate is placed on the worktable and has no clamp to restrict its movements. The speed of laser beam is considered constant and the time for laser to change direction is 4 second. The powder addition onto the substrate is divided into many small time steps to simulate the quasi-steady nature of LENS process.

**3.4 Transient thermal analysis**

Thermal conductivity and specific heat are temperature dependent. The heat transfer considered here is conduction, the effect of convection is considered & radiation are not considered. The latent heat required during phase change of SS 304 is also taken in to account. The element birth/death option is used to account for the addition of new elements in the solution domain corresponding to the deposition of powder for creating a multi-layer structure on a substrate. The substrate is assumed to serve simply as a heat sink. Boolean features of ANSYS is used for bonding of substrate and layers of thin wall. Thermal and Mechanical properties of SS304 is used for thin wall and substrate.

**3.5 Model**

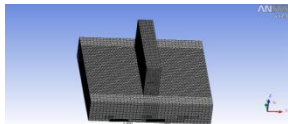


**Figure. 2 : Mesh and Nodes Generation**

A model for LENS process is built. As shown in Figure 4, Substrate : 40 x 40 x 10 mm. The example under consideration thin wall has length L=30 mm, breadth W=6 mm, height H=14 mm respectively. 6 tracks across width is assumed of equal width of 1 mm while each of the 20 layers in the wall height is assumed of equal 0.7 mm height . Each layer : 30 mm Long, 1 mm Wide and 0.7 mm height. As shown in Figure 2, a total of 25402 nodes, and 14951 Tetrahedral elements are generated to accomplish this simulation. The laser beam travel time for one pass is 4 seconds and it is discretized into 20 equal time steps with 0.20 second for each step. One more step with time t=200s is added after the existing 20 steps to account for the cooling after laser beam goes past the substrate.

**5 Layers**

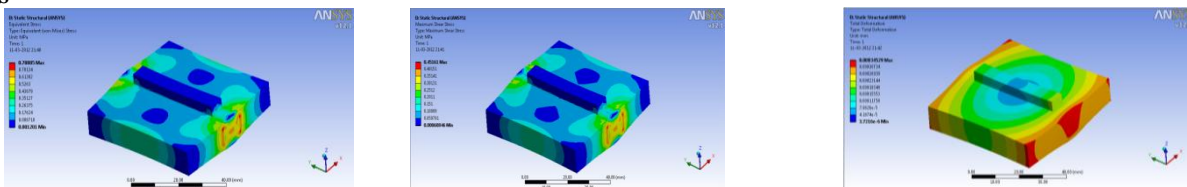


**Figure 3 : Von-mises stress distribution, Max. shear stress distribution and Total deformation**

**IV. Modelling consideration**

**4.1 Thermal boundary and initial condition**

The substrate is at room temperature as the beginning of the process and the ambient temperature  $T_0 = 20\text{ }^\circ\text{C} = 293\text{ K}$ . The side and top surface is assumed to be convection heat transfer with a constant coefficient of  $30\text{ W/m}^2\text{K}$ . The equivalent convection coefficient is  $400\text{ W/m}^2\text{K}$  for the bottom of substrate. Step applied for various temperatures as T or  $T_\infty$  as shown in below table.

**Table 1: Properties of SS304**

Temperature, T(°c)	Thermal Conductivity, $W.m^{-1}k^{-1}$	Yield Stress $\sigma_Y$ (MPa)	Young's modulus, E (GPa)	Latent Heat of Fusion, J/kg
25	14.8	241	193	-
400	20.7	159	-	-
600	23.5	134	-	-
800	25.8	114	-	-
1000	28.8	97	-	-
1100	29.9	-	-	-
1200	31.6	88	-	-
1300	32.8	76	-	-
1454	-	-	-	$2.65 \times 10^5$

**4.2 Structural boundary and initial conditions**

The substrate is assumed to be stress free at the beginning of the process. The only load applied to the system is the thermal field, analyzed in the previous step. The bottom of the substrate is subjected to displacement constraints so that it has no movement in the z direction. The substrate, however, is free to deform in the x and y direction.

**V. Simulation results**

**5.1 Temperature Distribution**

In the actual production, the LENS is a multi-track and multi-layer manufacturing process. In this analysis , the laser power is 3.0 kW, the scanning rate is  $14\text{ mm S}^{-1}$ , the speed of delivering powder is  $0.002\text{ kg S}^{-1}$ , the temperature field distribution after the laser returns, and the temperature field whose maximum temperature is 2038.77 K, lowest temperature is 20.00 K, and the temperature drops very quickly. The temperature distribution of the material right after finishing the last step of the deposition for each deposition pattern. The maximum temperature, just after turning off the laser, significantly drops below the melting temperature

**10 Layers**

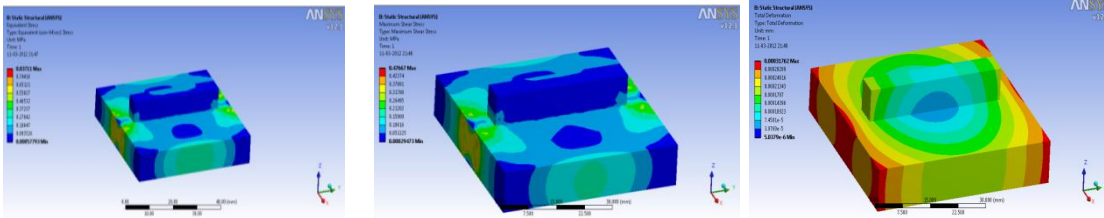


Figure 4: Von-mises stress distribution, Max. shear stress distribution, Total deformation distribution  
 15 Layers

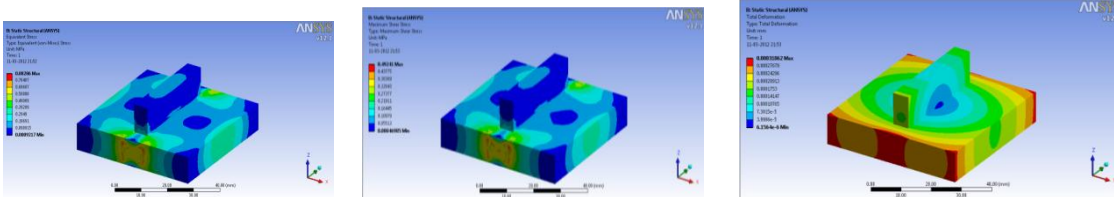


Figure 5 : Von-mises stress distribution, Max. shear stress distribution and Total deformation distribution  
 20 Layers

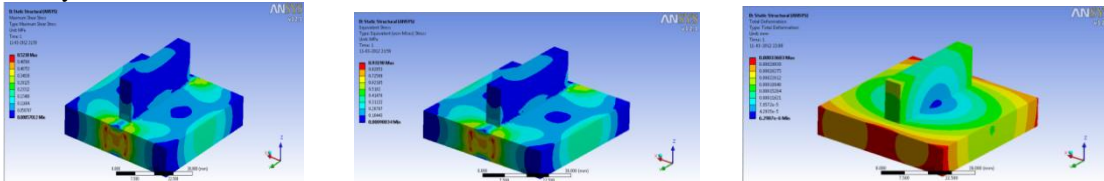


Figure 6 : Von-mises stress distribution, Max. shear stress distribution and Total deformation distribution

**VI. Results and discussion**

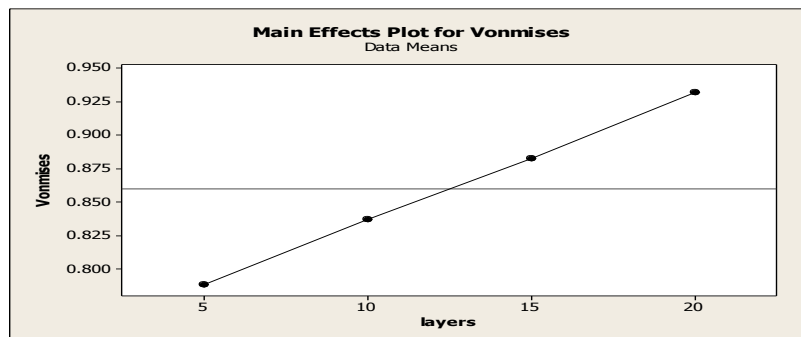


Figure 7 : Relation between layers and max. von-mises stress

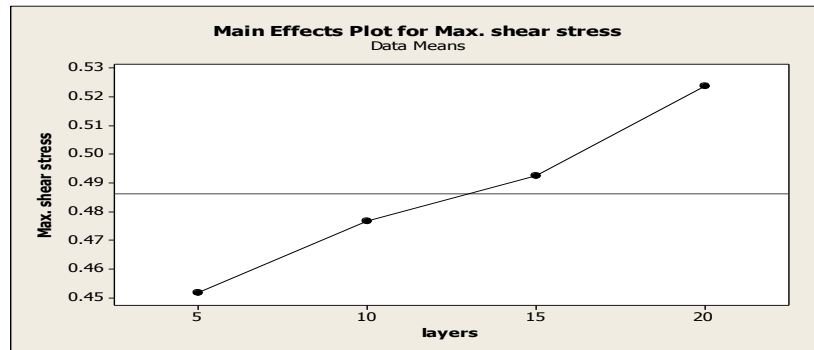


Figure 8 : Relation between layers and max. shear stress

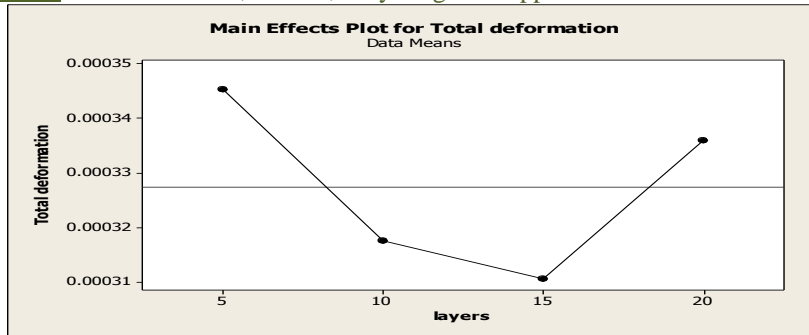


Figure 9: Relation between layers and max. total deformation

Table 2 : Result obtained for 5, 10,15 and 20 layers

		Location
Von-mises	Maximum	Substrate
	Minimum	Thin wall
Shear stress	Maximum	Substrate
	Minimum	Thin wall
Total deformation	Maximum	Substrate
	Minimum	Thin wall

As predicted, the thermal analysis of the process shows that the various deposition layers directly changes the temperature history of the process. The non-uniformity of the temperature field is one of the main reasons for stress rising. Figure 7 shows the Von-Misses stress at the end of the deposition process for each deposition pattern and the maximum Von-Misses stress value in various deposition layers . Among all deposition layers. The maximum stress occurs at the interface of the deposited material and the substrate. In order to better analyze the stress distribution of the deposited material, the Von-Misses stress of the surface of the deposited material is shown in above graph and as shown figure 8 as the layer increases the max. shear stress value also increases but as shown in figure 9 the total deformation is suddenly goes down and reaching up due to deposition strategy and sudden effect of laser power.

**VII. Conclusion**

Although in the different layers have different activated time, they have similar temperature and thermal stress variation regularities. The temperature gradients in specimen are mainly along Z direction, Among all those force components of Von Mise’s effective stress, Z -directional thermal stress is much larger. In the different layers, the Von Mise’s effective, total deformation, shear stress in next layer are almost twice the values of previous layer. The start point of each layer has an enormous effect on the distribution and intensity of thermal stress. During LENS, high thermal gradients tend to develop in the through-thickness direction. The associated differential thermal contraction often generates relatively high stresses, which are likely to cause yielding in the hot, near-surface regions. The present work has manifested that the peak temperature at any point is

attained when the laser beam passes over that location. As the beam moves away from the location, the newly deposited metal rapidly solidifies at a varying cooling rate with a very high initial value. During the deposition of subsequent layers the temperature again shoots up as the laser beam passes over the similar locations thus resulting in repetitive thermal cycles that can be correlated with the effect of gradual increment in total deformation, von-mises stress and shear stress.

**VIII. ACKNOWLEDGEMENTS**

I would like to express my deep sense of gratitude and respect to my guide Prof. R.I.Patel sir for his excellent guidance, suggestions and constructive criticism. I consider myself extremely lucky to be able to work under the guidance of such a dynamic personality. I am also thankful to A.H.Makwana sir for his co-operation throughout the semester.

**REFERENCES**

[1] Vilar, R. J. Laser Cladding. Laser Appl. Vol 11. No 2. 1999. Pp. 64-79.  
 [2] Atwood, C., Griffith, M., Harwell, D., Reckaway, D., Ensz, M., Keicher, D., Schlienger, M., Romero, M., Oliver, M., Jeanette, F., Smurgeresky, J. Laser Spray Fabrication for Net-Shape Rapid Product Realization LDRD. Sandia Report.1999.  
 [3] Sandia National Laboratories website.  
 [4] Griffith, M., Ensz, M., Puskar, J., Robino, C., Brooks, J., Philliber, J., Smurgeresky, J., Hofmeister, W. Understanding the microstructures and properties of components fabricated by laser engineered net shaping(LENS). Mat. Res. Soc. Symp. Proc. Vol 625. Warrendale, PA. 2000. Pp. 9-21.  
 [5] Keicher, D. Jellison, J., Schanwald, L., Romero, J. Towards a reliable laser spray powder deposition system through

- process characterization. 27th Int. Tech. Conf. Soc. Adv. Mat. Pro. Eng. Albuquerque, NM. 1995. Pp. 1009-1018.
- [6] Hofmeister, W., Wert, M., Smurgesky, J., Philliber, J., Griffith M., Ensz, M. Investigating solidification with the laser-engineering net shaping (LENSTM) process. JOM-e.
- [7] Hofmeister, W., Griffith, M., Ensz, M., Smurgesky, J. Solidification in direct metal deposition by LENS processing. JOM. Vol.53. No 9. 2001. Pp. 30-34.
- [8] Hofmeister, W., MacCalum, D., Knorovsky, G. Video monitoring and control of the LENS process. American Welding Society 9th International Conference of Computer Technology in Welding. Detroit, MI. 1998. Pp. 187-196.
- [9] Smugeresky, J., Keicher, D., Romero, J., Griffith, M., Harwell, L. Laser engineered net shaping (LENSTM) process: optimization of surface finish and microstructural properties Proc. of the World Congress on Powder Metallurgy and Particulate Materials. Princeton, NJ. 1997. Part 21.
- [10] Kahlen, F.-J., Kar, A. J. Tensile strengths for laser-fabricated parts and similarity parameters for rapid manufacturing. Manuf. Sci. Eng. Vol 123. No 1. 2001. Pp. 38-44.
- [11] Rangaswamy, P., Holden, T., Rogge, R., Griffith, L. J. Residual stresses in components formed by the laser-engineered net shaping (LENS®) process. Strain Analysis. Vol 38. No 6. 2003. Pp. 519-528.
- [12] Rangaswamy, P. Griffith, M., Prime, M., Holden, T., Rogge, R., Edwards, J., Sebring, R. Residual stresses in LENS® components using neutron diffraction and contour method. Mat. Sci. Eng. A. Vol 399. 2005. Pp. 72-83.
- [13] Riqing, Y., Smugeresky, J., Zheng, B., Zhou, Y., Lavernia, E. Numerical modeling of the thermal behavior during the LENS® process. Mat. Sci. Eng. A. Vol 428. 2006. Pp. 47-53.
- [14] Lindgren, L.-E. Finite element modeling and simulation of welding part : increased complexity. Journal of Thermal Stresses. Vol 24. 2001. Pp. 195-231.
- [15] Wang, L., Felicelli, S. Analysis of thermal phenomena in LENS™ deposition. Mater. Sci. Eng. A. Vol 435-436. 2006. Pp. 625-631.
- [16] Neela, V., De, A. Numerical modeling of LENS™ process using special element features. 2007 Abaqus India Regional Users' Meeting. 2007.
- [17] Deus, A., Mazumder, J. Two-dimensional thermo-mechanical finite element model for laser cladding. Proc. ICALEO. Duley, W., Shibata, K., Poprawe, R., eds. Orlando, FL. Laser Institute of America. 1996. Pp. B/174-B/183.
- [18] Labudovic, M., Hu, D., Kovacevic, R. A three dimensional model for direct laser metal powder deposition and rapid prototyping. J. Mat. Sci. Vol 38. 2003. Pp. 35-49.